

Original Paper

Titanium Dioxide Nanoparticle (TiO₂ NP) Induces Toxic Effects on LA-9 Mouse Fibroblast Cell Line

Ana Carolina M. Fattori^a Patrícia Brassolatti^a Karina A. Feitosa^a
Matheus Pedrino^a Ricardo de O. Correia^a Yulli R. Albuquerque^a
Joice M. de A. Rodolpho^a Genoveva L. F. Luna^a Juliana Cancino-Bernardi^{b,e}
Valtencir Zucolotto^b Carlos Speglich^c Karina N. Z. P. Rossi^d
Fernanda de F. Anibal^a

^aLaboratório de Inflamação e Doenças Infecciosas, Departamento de Morfologia e Patologia, Universidade Federal de São Carlos, São Carlos, SP, Brazil, ^bGrupo de Nanomedicina e Nanotoxicologia, Instituto de Física de São Carlos, Universidade de São Paulo, São Carlos, SP, Brazil, ^cCentro de Pesquisas, Desenvolvimento e Inovação Leopoldo Américo Miguez de Mello (CENPES/Petrobras), Rio de Janeiro, RJ, Brazil, ^dLaboratório de Patologia e Biocompatibilidade, Departamento de Morfologia e Patologia, Universidade Federal de São Carlos, São Carlos, SP, Brazil, ^eDepartamento de Química, Faculdade de Filosofia, Ciências e Letras de Ribeirão Preto, Universidade de São Paulo, Ribeirão Preto, SP, Brazil

Key Words

Nanotoxicology • *In vitro* • Titanium dioxide nanoparticle • Cytotoxicity • Oxidative stress

Abstract

Background/Aims: Titanium dioxide nanoparticles (TiO₂ NPs) are extensively applied in the industry due to their photocatalytic potential, low cost, and considerably low toxicity. However, new unrelated physicochemical properties and the wide use of nanoparticles brought concern about their toxic effects. Thereby, we evaluated the cytotoxicity of a TiO₂ NP composed of anatase and functionalized with sodium carboxylate ligands in a murine fibroblast cell line (LA-9). **Methods:** Scanning Electron Microscopy (SEM), Dynamic Light Scattering (DLS), and ATR-FTIR spectroscopy were applied to determine nanoparticle physicochemical properties. The cell viability (MTT assay) and clonogenic survival were analyzed in fibroblasts exposed to TiO₂ NP (50, 150, and 250 µg/mL) after 24h. Moreover, oxidative stress, proinflammatory state, and apoptosis were evaluated after 24h. **Results:** TiO₂ NP characterization showed an increased hydrodynamic size (3.57 to 7.62 nm) due to solvent composition and a heterogeneity dispersion in water and cell culture media. Also, we observed a zeta potential increased from -20 to -11 mV in function of protein adsorption. TiO₂ NP reduced fibroblast cell viability and induced ROS production at the highest concentrations (150 and 250 µg/mL). Moreover, TiO₂

NP reduced the fibroblasts clonogenic survival at the highest concentration (250 µg/mL) on the 7th day after the 24h exposure. Nevertheless, TiO₂ NP did not affect the fibroblast proinflammatory cytokines (IL-6 and TNF) secretion at any condition. Early and late apoptotic fibroblast cells were detected only at 150 µg/mL TiO₂ NP after 24h. **Conclusion:** Probably, TiO₂ NP photocatalytic activity unbalanced ROS production which induced apoptosis and consequently reduced cell viability and metabolic activity at higher concentrations.

© 2023 The Author(s). Published by
Cell Physiol Biochem Press GmbH&Co. KG

Introduction

Nanoparticles are synthesized particles, which sizes range from 1 to 100 nm with properties that differ from the source materials ("bulk" solid or extended solid) [1]. The study of these structures and molecules on a nanoscale comprises nanoscience, and their practical application in processes and products defines what we know as nanotechnology. Two of the premises that define nanotechnology are the nanoscale, in at least one of its components, and novelty, that is, modifications in many particle properties due to the nanoscale [2].

An important characteristic that nanoparticles have is a large surface area per unit volume when compared to larger diameter particles, which increases the number of atoms available on the surface of these nanomaterials. As such, these particles have new physical-chemical properties compared with same materials at the micro and macro scale [3]. This potentiation in optical, mechanical, electrical, and magnetic properties makes nanoparticles be used in several areas such as the petrochemical industry, biomedical applications, food storage and processing, construction, among others [4–6].

TiO₂ nanoparticles (TiO₂ NPs) can be originated from one of the three best-known crystalline forms of this mineral: anatase, rutile, and brookite. Studies indicate that the anatase form is more widely used commercially due to its higher catalytic activity when compared to rutile [7–10]. TiO₂ NPs have been widely used in recent years in the industry and consumer products, such as in the production of paints, paper, plastics, and cosmetics, due to their high catalytic activity when compared to fine particles of the same composition [3, 11].

Another potential TiO₂ NP use is in the energy field, especially in the oil and gas industry [12]. Overall, nanoparticles are used as an alternative to traditional surfactants due to their chemical stability at high salinity, temperature, and pressure. Thus, TiO₂ NPs can reduce the water/oil interfacial tension (IFT) and contact angle and increase the oil yield recovery from 22% by conventional methods to 54%, which brings a significant advance to the industry [13, 14]. Among other applications, TiO₂ NPs have a photocatalytic activity that enables the decomposition of organic compounds in wastewater at refineries [15, 16], and can be used for liquefied petroleum gas sensing [17]. The TiO₂ NP, the subject of this work, was synthesized to be applied in the oil industry and surface-modified with sodium carboxylate ligands that have surfactant function, which in addition to stabilizing the nanofluids, also increases considerably its solubility [18].

The TiO₂ NPs are usually considered to be poorly soluble and low toxic [3]. However, in the case of nanoparticles, the smaller the particle, the higher the concentration of atoms on its surface, which makes it more reactive [1]. This characteristic makes NPs very important for certain applications, however, they can present unique bioactivity, presenting a greater interaction with the organism, which brings challenges concerning human health and the environment [1, 3]. And exposure to these nanomaterials during preparation must be evaluated regarding the risks that their production may bring to handlers.

Several studies have shown that TiO₂ NPs exhibit higher toxicity when compared to particles that do not have a nanometric scale, which is associated with the most significant toxic effects among smaller particle sizes [3, 19, 20]. Size is a very important characteristic since NPs can be internalized and trigger a toxic response to the cellular system [21–24]. Besides possible internalization, NPs can induce pores in the cell membrane, or even the destruction of the cell membrane and organelles, and also bind to macromolecules, altering their structure and function, causing damage to cell function and communication [25, 26].

The main mechanisms of cytotoxicity of NPs are related to oxidative stress, inflammatory process, damage to DNA and organelles, which causes decreased metabolic activity, and cell death [23, 26]. The cell death that is triggered due to exposure to TiO₂ NPs can occur through various mechanisms such as apoptosis, necrosis, necroptosis which is characterized as programmed necrosis that involves binding to TNF (tumor necrosis factor), imbalance of the autophagy process that contributes to cellular homeostasis, as well as eryptosis in which erythrocyte death occurs [27–29].

An important mechanism that can trigger the apoptosis process and consequent cell damage is the reactive oxygen species (ROS) production. NPs can induce oxidative stress through direct ROS generation due to their physicochemical properties, by stimulating inflammatory cells to produce ROS, indirectly through changes in mitochondrial integrity, or ROS generation due to ions or soluble components of certain types of NPs [27]. Studies using fibroblasts and hepatocytes showed significant ROS production, DNA damage, and a high percentage of apoptotic cells after exposure to TiO₂ NPs [23, 24, 30, 31]. Kim and co-workers demonstrated that TiO₂ NPs induce oxidative stress via induction of prooxidant enzymes and suppression of antioxidant enzymes [32], and Gholinejad and colleagues suggested that TiO₂ NPs induce mitochondrial dysfunction which would be the initial source of ROS production generating oxidative stress [33].

Although many studies on nanotoxicity are produced every year [23, 24, 34–38], the mechanisms that trigger cytotoxicity are not yet fully elucidated. Moreover, the cellular effects of NPs are dependent on several factors, such as particle size, surface ligands, their agglomeration state, as well as the dose and exposure time in addition to the cell line being studied [3, 22, 26].

Thus our work evaluated the cytotoxic effects on LA-9 fibroblasts, a lineage still poorly studied regarding NP toxicity, after exposure to TiO₂ NP of greatly reduced size, composed of anatase and functionalized with sodium carboxylate ligands, being analyzed the acute exposure (24h). In addition, long-term effect after acute exposure was evaluated by clonogenic assay, not yet reported in the literature for this TiO₂ NP in LA-9 lineage. The representative scheme of the methods and results reported in this work after exposure of LA-9 fibroblasts to TiO₂ NP is presented in Fig. 1. It is expected that this work will provide fundamental data for the evaluation of the safety of manipulators in the production of this, as well as in the use of this TiO₂ nanoparticle, as a potential and important material for use in the petrochemical industry (PETROBRAS) in the oil extraction process.

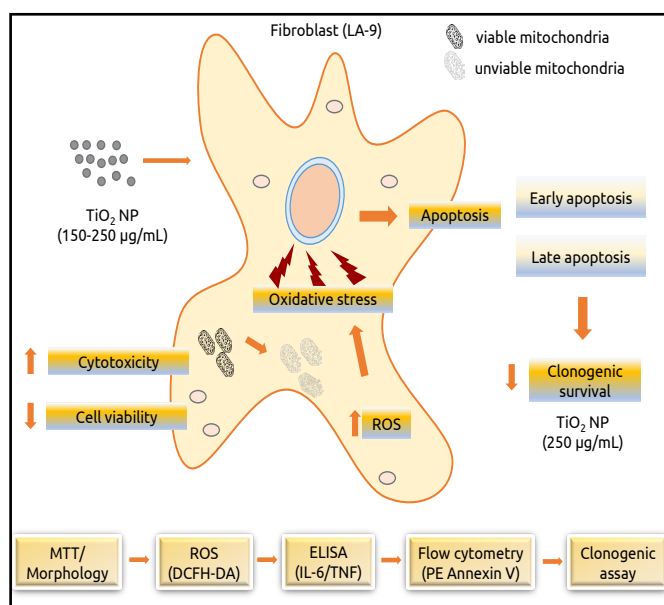


Fig. 1. Experimental design and effects triggered by exposure of TiO₂ NP in Fibroblasts LA-9.

Materials and Methods

TiO₂ NP characterization

TiO₂ NP was provided by CENPES - PETROBRAS (Centro de Pesquisas, Desenvolvimento e Inovação Leopoldo Américo Miguez de Mello). TiO₂ NP synthesis was based on anatase titanium dioxide followed

by functionalization with the ligand sodium carboxylate. The TiO₂ NP characterization was performed by Dynamic Light Scattering (DLS), Zeta Potential, Attenuated Total Reflectance Fourier Transformed Infrared (ATR-FTIR) spectroscopy and Scanning Electron Microscopy (SEM). The hydrodynamic diameter and zeta potential of the TiO₂ NP suspended (0.2 mg/mL) in ultrapure water (resistance > 18 MΩ·cm⁻¹ Mega Purity purification system - Thermo Fisher Scientific, Waltham - Massachusetts, USA) and in DMEM culture medium were evaluated using a Malvern spectrometer Nano-ZS (Malvern Instruments, Malvern, UK). The results are presented as mean ± SD resulting from three different measurements. Polydispersity index value (PDI) was also described. The Infrared spectra were obtained to evaluate the chemical surface group at the TiO₂ NP. In this work the Attenuated Total Reflectance Fourier Transformed Infrared (ATR-FTIR) spectroscopy was performed on a Bruker Alpha-P instrument (Germany) equipped with diamond crystal windows as the reflective element of the 4 mm². The sample was analyzed in the solid phase and the measurement was performed at a resolution of 4cm⁻¹ and considered 128 scans. The raw ATR-FTIR spectra data were analyzed by OMNIC 8.2 software (Thermo Fisher Scientific) to determine the wavelength of peaks. For SEM analysis, image acquisition was performed with a Philips – XL30 FEG (Amsterdã, Netherlands) electron microscope.

Cellular system

LA-9 (mouse fibroblast cells) were acquired from the Rio de Janeiro Cell Bank (BCRJ-Brazil - code 0142). The cell culture was maintained using Dulbecco's Modified Eagle Medium (DMEM - Sigma-Aldrich, St. Louis - Missouri, USA) supplemented with 10% fetal bovine serum (FBS - LGC Biotecnologia, Cotia - SP, Brazil) and 1% antibiotic (streptomycin/penicillin - LGC Biotecnologia). The fibroblasts were maintained in sterile T-75 flasks (Kasvi, São José dos Pinhais - PR, Brazil) and incubated at 37°C in a 5% CO₂ atmosphere.

Cell viability and morphology

The cell viability was determined with MTT (3-(4, 5-Dimethylthiazol-2-yl)-2, 5-Diphenyltetrazolium bromide) assay by which it is possible to evaluate mitochondrial enzymatic activity [39]. A preliminary test was performed using concentrations of TiO₂ NP ranging from 0.1 to 5000 µg/mL, in agreement with the literature and to check the toxicity of NP broadly [20, 40–44]. After initial testing, concentrations of 50, 150, and 250 µg/mL were chosen for the study. LA-9 fibroblasts were seeded in a 96-wells plate at a density of 6x10³ cells/well and cultivated at 37 °C in a 5% CO₂. After 24h of incubation to adhesion of cell, the cell culture was exposed to TiO₂ NP at 50, 150, and 250 µg/mL for 24h. The positive control was considered as cells exposed to a solution of Extran 5% (Merck, Darmstadt, Germany) and the negative control was only cells cultured using DMEM. After the exposure to the different concentrations of TiO₂ NP, microphotographs were taken to observe the morphology of the fibroblasts using an optical microscope (Zeiss, Oberkochen, Germany) at 100x magnification. Subsequently, the supernatant was removed and was added 100 µL of MTT solution (0, 5 mg/mL) for 4h (Sigma-Aldrich). After this period, the supernatant was removed and 100 µL of DMSO (Synth, Diadema – SP, Brazil) was added to solubilize formazan crystals. The absorbance was measured at 570 nm (Thermo Scientific - Multiskan GO spectrophotometer). The cell viability (%) was calculated considering the mean of the negative control group as having 100% of cell viability. To do this, the mean absorbance of the group exposed to TiO₂ NP is divided by the mean absorbance of negative control and multiplied by 100. Three independent experiments were carried out in quadruplicate for cell viability and in triplicate for obtaining the images.

Clonogenic survival assay

This assay was performed according to Franken et al [45], in the 6-wells plate at a density of 100 cells/well, in a final volume of 2 mL of cell suspension in DMEM medium. After cell adhesion, exposure to the TiO₂ NP at 50, 150, and 250 µg/mL were performed for 24h, and in the negative control was used only DMEM. Subsequently, the supernatant was removed and the cells were washed with 1x PBS buffer, and 2 mL of fresh DMEM was added to the cells. The cell cultures were incubated for 7 days in the same condition previously described. After this period the culture medium was removed, and cells were fixed adding slowly 1 mL of cold methanol (Synth). Then, cells were stained using 1 mL of violet crystal solution 0.1% (Synth) at room temperature for 1 minute. Next, the wells were washed with distilled water. The wells were photographed, and the colonies were counted using the ImageJ 1.53a software. The plating efficiency (PE) was determined by dividing the number of colonies by the number of cells initially seeded and the survival fraction (SF) was calculated by dividing the mean PE of cells exposed to TiO₂ NP by the mean PE of the negative control. Three

independent experiments were performed in duplicate.

Measurement of reactive oxygen species (ROS) production

The intracellular reactive oxygen species (ROS) levels were measured using the fluorescent probe DCFH-DA (2',7'-Dichlorodihydrofluorescein Diacetate) as described by Wan et al. [46] and Wang and Joseph [47]. LA-9 fibroblasts were seeded in a 96-wells plate at a density of 1×10^4 cells/well. After the period of cell adhesion, the cells were exposed to TiO₂ NP at 50, 150, and 250 $\mu\text{g}/\text{mL}$ for 24h. To the negative control group only DMEM was used, and for the positive control group, the cells were exposed to 0.1 mM H₂O₂ solution (Dinâmica, Indaiatuba – SP, Brazil) 30 minutes before the addition of fluorescent probe. After 24h, the solution was removed and the cells were washed with 1x PBS and incubated with 100 μM of DCFH-DA (Sigma-Aldrich) solution for 30 minutes protected from light. After this period cells were washed with 1x PBS. The fluorescence analysis was performed at 485-530 nm (Spectra MAX i3 - Molecular Devices, San Jose, California, USA). The percentage of intracellular ROS production of experimental groups was calculated using the mean fluorescence emission of samples exposed to TiO₂ NP divided by mean fluorescence emission of the negative control and multiplied by 100. Three independent experiments were performed in quadruplicate.

Proinflammatory cytokines quantification

The fibroblasts (LA-9) were seeded on a 96-well plate at 1×10^4 cells per well and were incubated with TiO₂ NP (50, 150, and 250 $\mu\text{g}/\text{mL}$) for 24h. Following incubation, the supernatant was collected and the production of the IL-6 and TNF cytokines were determined by ELISA (Enzyme-Linked Immunosorbent Assay). The instructions were according to the manufacturer (BD Biosciences, New Jersey, USA). The absorbance was measured using a plate spectrophotometer (Multiskan GO) at 450 nm and the concentrations of the cytokines were calculated based on a standard curve. Results were expressed in pg/mL and three independent experiments were carried out in triplicate.

Cell death assay

Flow cytometry analysis was used to evaluate the cell death mechanism of fibroblasts LA-9 by PE Annexin V detection (BD Biosciences) after exposure to TiO₂ NP (50, 150, and 250 $\mu\text{g}/\text{mL}$) for 24h. LA-9 cells were seeded on 24 wells-assay plates at the density of 1×10^5 cells/well. After 24h, the plates were centrifuged (1500 rpm at 4°C for 10 minutes) and washed with 1x PBS. Then, antibodies PE Annexin V and 7AAD (7-Aminoactinomycin D) [1:1] (1 $\mu\text{L}/\text{well}$ in 1:10 binding buffer) were added. The reaction lasted 15 minutes at room temperature protected from light. Then, the cells were removed with the aid of a scraper and resuspended in microtubes with 300 μL of binding buffer. Camptothecin (Sigma-Aldrich) 500 $\mu\text{M}/\text{well}$ was used as a positive control. Analyzes were performed on a flow cytometer on an Accuri™ C6 BD Biosciences, selecting a gate with 10,000 events using FlowJo™ software version XV (BD Biosciences). Two independent experiments were carried out in quadruplicate. The data is demonstrated by a representative dot plot where Q1 – necrotic cells (PE - / 7AAD +), Q2 – late apoptosis (PE + / 7AAD +), Q3 – viable cells (PE - / 7AAD -) and Q4 – early apoptosis (PE + / 7AAD -).

Statistical analysis

The results were expressed as mean \pm standard deviation (SD) and analyzed in GraphPad Prism software, version 7 – 2018 (San Diego, CA, USA). Shapiro-Wilk, Kolmogorov-Smirnov, or D'Agostino & Pearson normality tests were applied depending on the number of samples analyzed. Subsequently, for parametric data, the One-way ANOVA test (One-way Analysis of Variance) and Tukey's post-test (Tukey's Multiple Comparison Test) were used. For non-parametric data, the Kruskal-Wallis test and Dunn's post-test (Dunn's Multiple Comparison Test) were used. Statistical significance was established at p values < 0.05.

Results

Nanoparticle characterization (TiO₂ NP)

The characterization of TiO₂ NP in ultrapure water and DMEM media is presented in Table 1. The hydrodynamic diameter of TiO₂ NP in water was about 3.57 ± 1.97 nm. Zeta potential measures revealed a negative charge of -20 ± 3 mV in TiO₂ NP in water probably due to the coating with carboxylic acid ($-\text{COO}^-\text{Na}^+$). We suggested that dispersion of TiO₂

Table 1. Hydrodynamic diameter, Pdl and Zeta potential values of TiO₂ NP in ultrapure water and DMEM culture medium

TiO ₂ NP suspension	Hydrodynamic diameter (nm)	Pdl	Zeta potential (mV)
Ultrapure water	3.57 ± 1.97	0.548 ± 0.121	-20 ± 3
DMEM	7.62 ± 0.59	0.553 ± 0.064	-11 ± 2.6

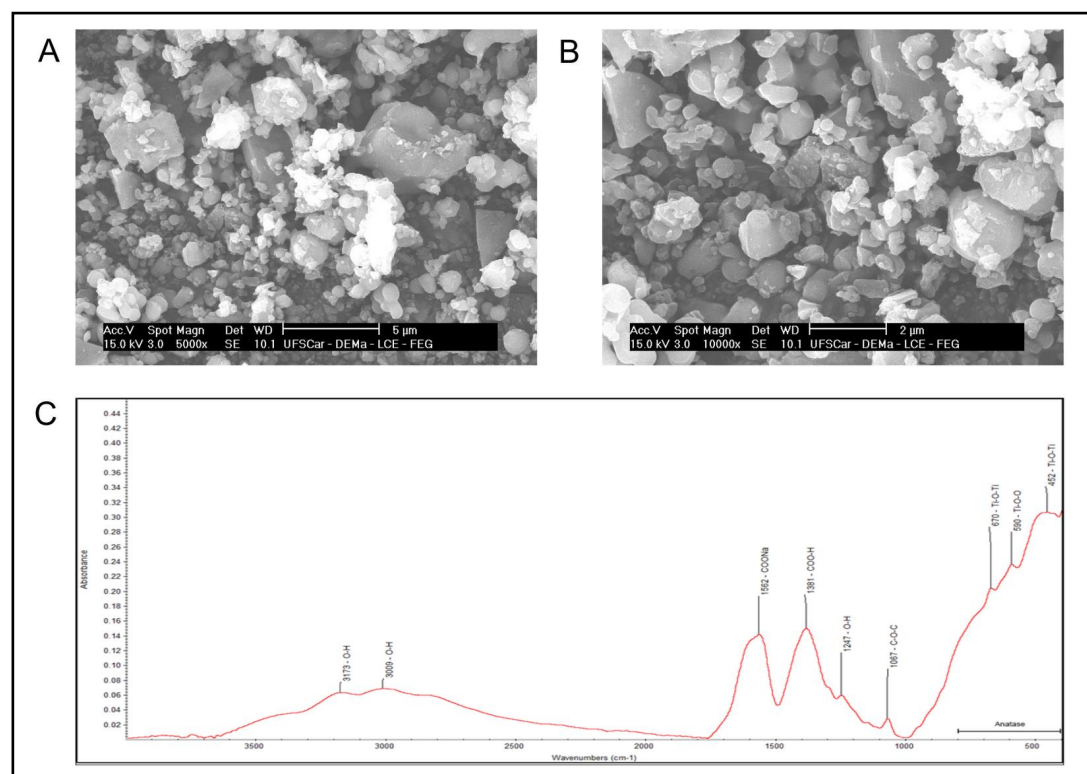


Fig. 2. SEM microscopy images of anatase structures in TiO₂ NP at 5000x (A) and 10000x (B) and ATR-FTIR spectroscopy of the TiO₂ NP (C).

NP in DMEM media induced some nanoparticle aggregation or protein corona formation on its surface, as showed by the increase of the hydrodynamic diameter to 7.62 ± 0.59 nm. Furthermore, zeta potential increases to -11 ± 2.6 mV in function of protein adsorption. Interesting that both solvents revealed polydisperse index values around 0.5 an indicative of heterogeneity dispersion as observed by SEM images in Figures 2A and 2B.

The ATR-FTIR spectrum obtained from TiO₂ NP shows peaks at 452; 590; 670; 1067; 1247; 1381; 1562; 3009, and 3173 cm⁻¹, Fig. 2C. These peaks can be associated with some groups presented in TiO₂ NP which are discussed later.

Cytotoxicity and morphology of LA-9 fibroblasts

The MTT assay of fibroblasts after 24h exposure to TiO₂ NP showed an indicative of cytotoxicity as there was a reduction in the percentage of cell viability at the highest concentrations, 150 µg/mL (34.4% ± 12.77 – 65.60% reduction) and 250 µg/mL (43.79% ± 13.96 – 56.21% reduction) when compared to the negative control group (100% ± 11.38), Fig. 3A.

According to cell morphology, it is possible to notice that fibroblasts exposed at 150 µg/mL and 250 µg/mL TiO₂ NP (Fig. 3D and 3E), showed a lower level of elongated cells (characteristic morphology of the fibroblast cell), which now have a more rounded shape when compared to control group, which has normal cell morphology and growth, Fig. 3B.

Furthermore, it is possible to observe an accumulation of TiO₂ NP at the bottom of the well, Fig. 3D and 3E, which was not observed in the control group, Fig. 3B and also at the lowest concentration of 50 µg/mL, Fig. 3C, which showed no reduction in the percentage of cell viability.

Additionally, we performed the clonogenic survival assay, Fig. 4, in which we observed the formation of fibroblasts cell colonies after 24h exposure to TiO₂ NP. The highest concentration (250 µg/mL) showed a significant reduction in the number of colonies when

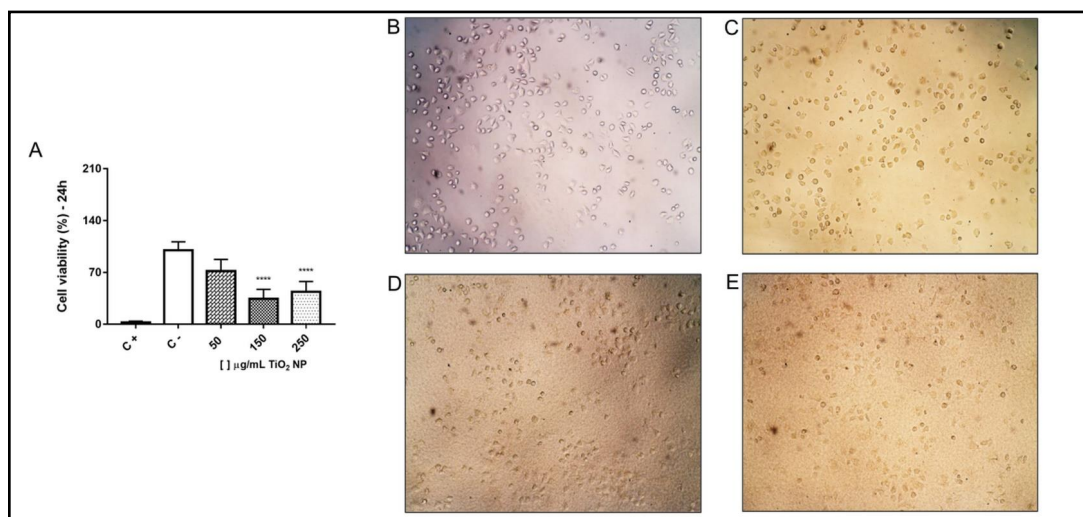


Fig. 3. Fibroblast LA-9 cell viability (%) after exposure to different concentrations of TiO₂ NP in the 24 hours (A) and representative of fibroblast LA-9 morphology from each experimental group (B – C-; C – 50 µg/mL; D – 150 µg/mL and E – 250 µg/mL). The amplification is 100x. C- is negative control and C+ is positive control (Extran™ 5%). Data represent mean ± SD from three independent measurements. The statistical analysis was performed by the Kruskal-Wallis non-parametric test and Dunn's post-test. Statistical significance ****p<0,0001 represents the difference between the results obtained in the groups exposed to different TiO₂ NP concentrations and the negative control group (C-).

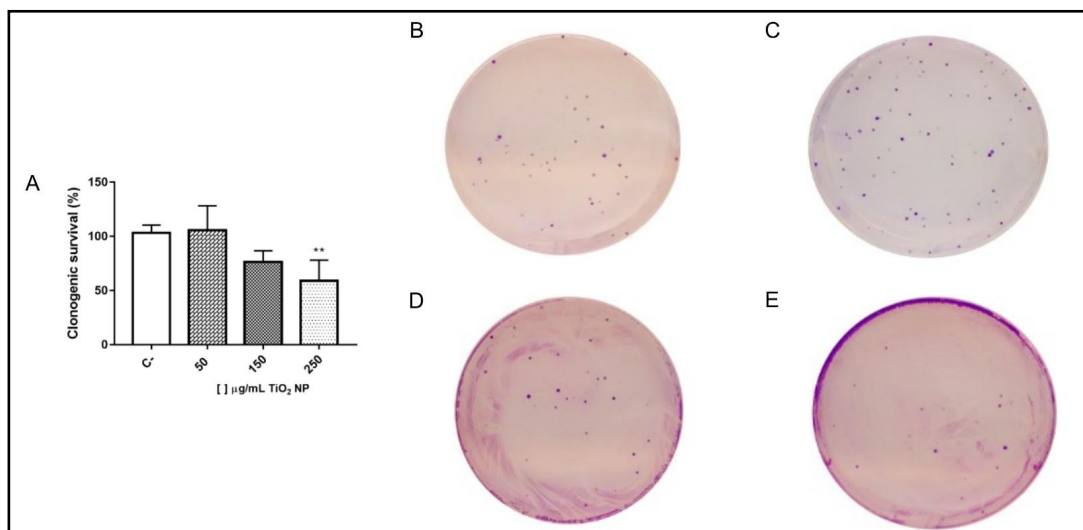


Fig. 4. Clonogenic survival (%) of LA-9 fibroblasts after exposure to TiO₂ NP for 24 hours (A) and representative of the wells containing the cell colonies from each experimental group (B – C-; C – 50 µg/mL; D – 150 µg/mL and E – 250 µg/mL). C- is negative control. The survival fraction was calculated using the average C- as 100% survival. Data represent mean ± SD from three independent measurements. The statistical analysis was performed by the One-way ANOVA parametric test and Tukey's post-test. There was no statistically significant difference between the results obtained in the groups exposed to the different concentrations of TiO₂ NP when compared to the negative control group (C-).

compared to the control group, Fig. 4A. Also, it is possible to observe in Figures 4B to 4E a representative of the wells showing colony formation in the experimental groups.

Oxidative stress

To evaluate oxidative stress, the percentage of reactive oxygen species (ROS) production was measured after exposure to TiO₂ NP for 24 hours. For concentrations of 150 and 250 µg/mL there was a significant increase in ROS production when compared to the negative control group which was not exposed to NP, Fig. 5.

Cytokines production – Inflammation

The pro-inflammatory cytokines IL-6 and TNF levels were dosed in the supernatant of fibroblasts after 24 hours of exposure to TiO₂ NP. For both cytokines, there was no significant difference between the groups exposed to NP and control group, Fig. 6.

Cell death

Flow cytometry was analyzed to investigate cell death induction in fibroblasts exposed to TiO₂ NP. The cells that were exposed to the concentration of 150 µg/mL showed a significant increase in the percentage of apoptotic cells when compared to the negative control group, not exposed, Fig. 7D. It was observed that in this same group (150 µg/mL) there is an increase in the percentage of apoptotic cells both early, Fig. 7B, and late, Fig. 7C. There was no increase in the percentage of necrotic cells for any of the NP-exposed groups when compared to the negative control group, Fig. 7E.

Fig. 5. Reactive oxygen species (ROS) production (%) on LA-9 fibroblasts after exposure to TiO₂ NP for 24 hours. C- is negative control and C+ is positive control (H₂O₂ 0.1 mM). Data represent mean ± SD from three independent measurements. The statistical analysis was performed by the Kruskal-Wallis non-parametric test and Dunn's post-test. Statistical significance *** p<0,001 and ** p<0,01 represents the difference between the results obtained in the groups exposed to different TiO₂ NP concentrations and the negative control group (C-).

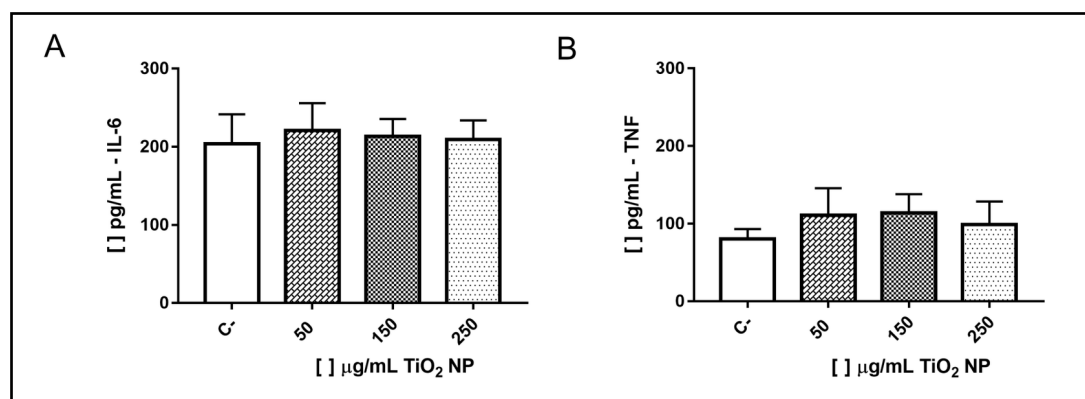
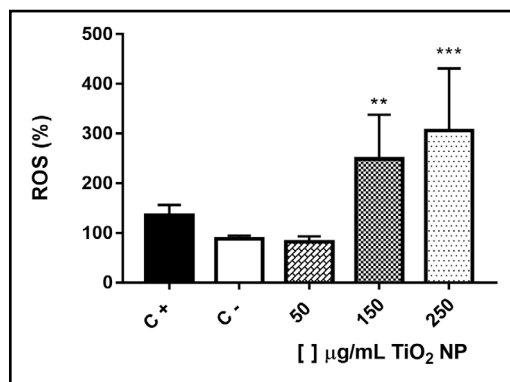


Fig. 6. Concentrations of IL-6 (A) and TNF (B) in pg/mL in the supernatant of LA-9 fibroblasts after exposure to TiO₂ NP for 24 hours. C- is negative control. Data represent mean ± SD from three independent measurements. The statistical analysis was performed by the One-way ANOVA parametric test and Tukey's post-test. There was no statistically significant difference between the results obtained in the groups exposed to the different concentrations of TiO₂ NP when compared to the negative control group (C-).

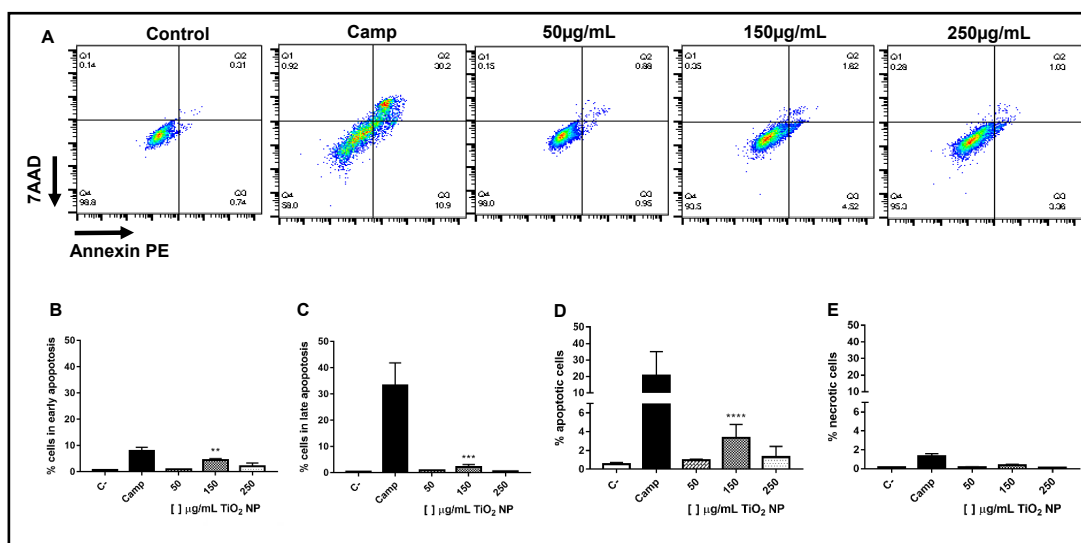


Fig. 7. Flow cytometry analysis to determine necrosis and apoptosis of LA-9 fibroblasts after exposure to TiO₂ NP for 24 hours. C- is negative control and Camp is positive control (Camptothecin 0.5 mM). (A) Representative two-dimensional contour density plots to determine fractions of live, necrotic and apoptotic cells; (B) Percentage of cells in early apoptosis; (C) Percentage of cells in late apoptosis; (D) Percentage of apoptotic cells (early + late apoptosis) and (E) Percentage of necrotic cells. Data represent mean \pm SD from two independent measurements. The statistical analysis was performed by the Kruskal-Wallis non-parametric test and Dunn's post-test. Statistical significance ** $p < 0,01$, *** $p < 0,001$ and **** $p < 0,0001$ represents the difference between the results obtained in the groups exposed to different TiO₂ NP concentrations and the negative control group (C-).

Discussion

The high and quick increase in the use of nanoparticles, especially in industry and consumer products, has brought concern about the need to study the safety of these new materials. Particularly TiO₂ NPs have been widely used due to their high catalytic activity, resulting in unique bioactivity and consequent concern for human health [3]. Thus this work aimed to evaluate the toxicity of TiO₂ nanoparticle (TiO₂ NP) functionalized with sodium carboxylate using the LA-9 fibroblast cell line as an *in vitro* model. This cytotoxicity evaluation was done through characterization of the nanoparticle and subsequent analysis of cell viability and morphology, ROS (oxidative stress) and pro-inflammatory cytokines production, cell death, and analysis of the long-term effect after acute exposure through cell colony formation.

The physicochemical properties of nanoparticles, such as crystalline shape, size, charge, and surface ligands, are closely related to the nanoparticle's biological effects [1, 3,26]. In addition, proteins from the medium can bind or be adsorbed onto the nanoparticle surface forming a structure called a protein corona, which can modify the physicochemical properties of the NPs and thus also interfere with cellular responses such as internalization, bioavailability, and toxicity [48, 49].

Both biological fluids and cell culture medium present free proteins that can bind to the NP surface [48]. This interaction and formation of the protein corona can be confirmed by changes in size and zeta potential of the NP [49]. Our results showed that the hydrodynamic diameter of TiO₂ NP increased from 3.57 nm in water to 7.62 nm in the DMEM medium. The fetal bovine serum (FBS) used to supplement the medium presents itself as a biological fluid that contains various proteins, which contribute to the corona effect [49]. Other authors also demonstrated the corona effect after dispersion in DMEM medium for the same TiO₂

NP [23] and gold particles [50]. Furthermore, it was observed that the dispersion of TiO₂ NP in DMEM medium was not stable based on PDI values around 0.5, an indication of the heterogeneous dispersion revealed in SEM images.

Despite the increase in size identified by aggregation and or corona protein formation, it is noted that this TiO₂ NP still presents a size considered small. NPs with sizes below 20-30 nm tend to have high reactivity due to an exponential increase of atoms on their surface, generating an excess of energy that makes them thermodynamically unstable [1]. Studies show that TiO₂ NPs can be internalized by cells and this mechanism is size and concentration-dependent, where NPs with sizes between 30-100 nm generally remain in the cell cytoplasm and NPs with sizes below 30 nm can reach the nucleus [31, 51].

Another interesting feature that interferes with the mechanism of uptake and consequent toxicity is the surface charge due to the interaction with phospholipid groups or protein domains present on the cell surface [48]. Positively charged NPs can interact more easily with these components [48, 52]. The zeta potential is an important physicochemical parameter of nanoparticles as it presents its charge and determines its properties in suspension [53], with NPs that exhibit values above ± 30 mV being considered stable [54]. The zeta potential revealed a negative charge of -20 mV on TiO₂ NPs in water probably due to binding with the carboxylic acid (-COO-Na⁺). Functionalization with carboxylic acid makes TiO₂ NPs more hydrophilic compared to particles without this functionalization thus changes in their bioactivity and consequent toxicity may occur [55]. Moreover, the zeta potential increased to -11 mV in TiO₂ NP suspended in DMEM as a function of protein adsorption. Both zeta potential values were associated with the aggregation/agglomeration tendency of TiO₂ NP as already reported by other authors [20, 43, 56, 57].

ATR-FTIR spectra were collected to elucidate the surface groups associated with TiO₂ NP [58]. The ATR-FTIR result shows typical broadband from 400 to 1000 cm⁻¹, related to Ti-O-Ti stretching vibration [59-61]. Moreover, in the spectrum were observed peaks around 452 and 670 cm⁻¹ in the same range, these peaks and ranges are regular to anatase TiO₂ [38]. Furthermore, a peak was reported at 590 cm⁻¹ and 670 cm⁻¹ which can be attributed to Ti-O-O bond and Ti-O-Ti respectively [62, 63]. The peak at 1067 cm⁻¹ is associated with C-O-C stretching vibration [64-66]. While the peak around 1247 cm⁻¹ represents O-H stretching vibration and this is a typical absorption region of hydrogen bond by carboxyl group and the hydroxyl group of anatase TiO₂ [67-69]. In the spectrum was observed peak at 1381 cm⁻¹, this region could be associated with carboxyl groups [60]. Moreover, the characteristic peak of COONa is around 1500 cm⁻¹, thus our result demonstrated a peak in the same region (1562 cm⁻¹) [70]. Carboxylic acids are in the group of molecules that are used in the functionalization of NPs that are of interest in the biomedicine area to promote greater biocompatibility [71-73]. Hamilton and co-workers demonstrated that TiO₂ NPs functionalized by carboxylation showed a reduction in toxicity [55]. The band from 3000-3600 cm⁻¹ is characterized by O-H stretching vibration of free and hydrogen-bonded surface hydroxyl groups [60, 69].

Cytotoxicity is related to the physicochemical characteristics of NPs and is dependent on the cell lineage of interest, the dose used, and the exposure time. Furthermore, biologically it is determined by significant modifications in cellular metabolism that can trigger oxidative stress processes and even death [26]. Our results, from the MTT assay, show that there was a reduction in cell viability of LA-9 fibroblasts for the highest concentrations, i.e., at the 250 µg/mL concentration we observed a 56.21% reduction in cell viability, and at the 150 µg/mL concentration, 65.60% reduction. Pedrino and co-workers [23] using the same TiO₂ NP at concentrations of 10, 100 and 1000 µg/mL and the same cell line observed reduced viability only at the 1000 µg/mL concentration. Since we are even dealing with the same cell line and the same TiO₂ NP, it is possible to suggest that there may be a toxicity threshold, since concentrations below and equal to 100 µg/mL do not show cytotoxicity and from 150 µg/mL onwards become toxic for the LA-9 fibroblast lineage. Other works in the literature corroborate our results as they also found reduced cell viability at concentrations close or equal after 24h of exposure to TiO₂ NP, such as reduction at the concentration of 100 µg/mL for hamster fibroblast lineage (V79) [42], reduction at the concentrations of 125 and 250

µg/mL for human astrocytoma lineage (D384) [43] and reduction at concentrations of 50 and 100 µg/mL for mouse preadipocyte lineage (3T3-L1) [44]. Jim and collaborators [40], on the other hand, observed no significant viability reduction within 24 hours but found this reduction within 48 hours at a concentration of 600 µg/mL, which may suggest that the cytotoxicity mechanism may occur in a dose and time-dependent manner.

In addition to altering mitochondrial metabolism, exposure to NPs can cause morphological changes in cells [26]. Fibroblasts are normally elongated cells in a fusiform shape, being adherent and growing in confluent monolayers [26, 74]. In our study, it was possible to observe that at the highest concentrations tested (150 and 250 µg/mL) morphological changes were detected as a rounded shape, which suggests a change in cell adhesion capacity corroborating our MTT results. In addition, it was possible to verify NP accumulation at the bottom of the wells of the culture plates for the same concentrations, already reported by Brassolatti and collaborators (2022).

This accumulation could impair the adhesion of fibroblasts on the plate and consequently cause changes in cell morphology that become more rounded instead of elongated cells. Ibrahim and co-workers reported that TiO₂ NPs impaired cell adhesion and cytoskeletal architecture of human osteoblast-like cells, and this effect was more significant in very small NPs of 5 nm [19]. Several authors have reported morphological changes in fibroblasts of various lineages, and also mesenchymal cells, after exposure to TiO₂ NP [19, 23, 24, 40, 42, 75–79]. Lee and co-workers (2018) corroborate our results in that at the concentration of 50 µg/mL the fibroblasts showed similar morphology to the control group, but the concentrations of 100 and 150 µg/mL showed lower cell density and changes in morphology.

One of the main cytotoxicity mechanisms associated with TiO₂ NP exposure is oxidative stress, which can trigger DNA damage and consequent cell death [48, 80]. Several authors have suggested that TiO₂ NP induces toxicity via oxidative stress and ROS production mainly, as it produces free radicals in suspension [24, 26, 48, 51, 80–82]. The results of our work showed that there was an increase in intracellular ROS production in LA-9 fibroblasts after 24h of exposure to TiO₂ NP at concentrations of 250 and 150 µg/mL. Pedrino et al [23], also demonstrated increased ROS production after 24h of exposure using the same TiO₂ NP, the same cell lineage, but at different concentrations (100 and 1000 µg/mL). In addition, they observed genotoxic effects starting at the concentration of 1 µg/mL, demonstrating that oxidative stress via ROS in this cell lineage can cause DNA damage associated with the size and crystalline form of the NP. Other studies also corroborate our results. The study by Gholinejad and collaborators [20] reported increased intracellular ROS production after 24h of exposure to TiO₂ NPs for the concentration of 100 µg/mL in human endothelial cells (HUVECs), but no change was found when the 50 µg/mL concentration was used, as presented in our study. Brassolatti and co-workers [24], using the same TiO₂ NP, found an increase in intracellular ROS production at the 100 µg/mL concentration but in human skin keratinocyte and fibroblast cell lines.

Furthermore, from the increased ROS generated by TiO₂ NP exposure, other changes are triggered such as gene induction and consequent secretion of inflammatory factors and expression of adhesion molecules, which are related to pro-apoptotic processes [20]. Studies have shown increased expression of inflammatory genes and secretion of pro-inflammatory factors, IL-6 and TNF, in endothelial cells after exposure to anatase TiO₂ NP [20, 83]. Fibroblasts are cells that act in the immune system and can increase IL-6 secretion under inflammatory conditions to amplify immunity [84]. In contrast to working with endothelial cells, our results showed that there was no increase in the secretion of either IL-6 or TNF by LA-9 fibroblasts after 24h exposure to TiO₂ NP. Bernier and co-workers [11] corroborate our results and also found no increase in IL-6 and TNF for the L929 mouse fibroblast lineage after 24 and 48h exposure to anatase TiO₂ NP. In contrast, in human keratinocyte (HaCaT) and fibroblast (HDFn) lineages lower IL-6 production was observed at the highest concentration tested after exposure to the same TiO₂ NP [24].

Although *in vitro* studies have demonstrated increased secretion of inflammatory factors and found a strong relationship of these results with the crystal structure of TiO₂ NP,

showing that anatase has a greater adjuvant role in the inflammatory process than rutile [20, 83, 85], our results and those of other authors demonstrate that the inflammatory profile must have a great relationship with the cell lineage in question [11, 24]. Furthermore, it should be noted that this TiO₂ NP was functionalized to reduce the risk of cytotoxicity which may have contributed to the non-induction of an acute inflammatory response. In this way, understanding which death mechanisms are associated with the cytotoxicity of this nanoparticle will add more information about the risks, helping to better define its toxic potential.

A final pathway to damage resulting from oxidative stress is the process of cell death usually resulting from apoptosis [26, 80, 86]. Apoptosis is a mechanism of programmed cell death that contributes to homeostasis, but can also occur as a defense mechanism in response to some cellular damage [87]. Our results showed that there was an increase in apoptotic cells after 24h of exposure to TiO₂ NP for the LA-9 fibroblast cell line at the 150 µg/mL concentration, and the same was not observed for the 250 µg/mL concentration, which showed reduced cell viability, morphological changes, and increased ROS production. Moreover, this increase was more expressive for cells in early apoptosis. Pedrino and co-workers [23], using the same TiO₂ NP and the same cell lineage, found an increase in early apoptotic cells for the 100 µg/mL concentration. Another study, using human endothelial cells (HUVECs) also reported an increase in early apoptotic cells for the 50 and 100 µg/mL concentrations after 24h of exposure to TiO₂ NP, but in the overall percentage of apoptotic cells, only the 100 µg/mL concentration continued to show this increase [20]. On the other hand, for human hepatoma cells (HepG2) an increase in both early and late apoptotic cells was demonstrated after 24h of exposure to TiO₂ NP at low concentrations [30].

Interestingly, early-stage apoptosis can be reversed when subjected to weak pro-apoptotic signals. Cells in early apoptosis that have been induced by p53 can have the apoptotic mechanism reversed if the stimulus that triggered this process is removed [87]. Our work, as well as others presented above, evaluated acute toxicity with 24h exposure only. It is suggested that DNA may undergo repair early in the p53-induced apoptotic process and that this repair may be responsible for the reversal of the cell death pathway in some circumstances [87].

We already know that this TiO₂ NP can impair fibroblasts LA-9 DNA [23]. However, there is a possibility of DNA repair and therefore the study was complemented by the clonogenic assay that evaluates the cell survival and proliferation capacity, from the formation of colonies, after 24h exposure to TiO₂ NP and subsequent withdrawal of this stimulus. It is also noteworthy that this assay is considered the gold standard among cytotoxicity assays due to its higher sensitivity [45, 88]. The results of our work demonstrate a significant reduction of colonies for the highest concentration evaluated (250 µg/mL), which indicates that exposure to TiO₂ NP at this concentration and for this cell line triggered cytotoxic aspects that were not corrected by the mechanisms mentioned above. In the other concentrations, no significant change in the number of colonies was observed ten days after acute nanoparticle exposure. This fact suggests that cells submitted to a concentration of 150 µg/mL of TiO₂ NP, which showed morphological changes and signs of apoptosis, were able to reverse the damage after NP removal, possibly through DNA correction pathways, which they became capable of recovering its intrinsic proliferation mechanisms through an adequate cell cycle. Similarly, Uboldi et al. (2016) also found no decrease in colonies for the 3T3 mouse fibroblast strain after 24h exposure to TiO₂ NP, however, they did demonstrate a reduction in colonies when the cells were exposed for 72h to rutile TiO₂ NP. For human skin (BJ) fibroblasts, no colony reduction was also observed after 24h of exposure to TiO₂ NP [88]. In contrast, Coccini and colleagues (2015) observed colony reduction in neuronal cells after prolonged exposure to low concentrations of TiO₂ NP. Through these reports, it can be considered that toxicity is related to both the cell type and the time and concentration used.

To date, there is no exact consensus on which parameters should be considered when classifying a nanoparticle as toxic or not, either for human health or the environment. Furthermore, it is important to highlight the difficulty in comparing the results present in

the literature due to the diversity of nanoparticles and their different characteristics, in addition to the different types of cell lines evaluated. Although the OECD (Organisation for Economic Co-operation and Development) does not yet have a specific guide for *in vitro* tests to evaluate the toxicity of nanoparticles, the methodology used in this work to determine cytotoxicity is presented as the most widely used by the literature [89].

From the results found in our work, it is possible to suggest that this TiO₂ NP has a cytotoxic effect on the LA-9 mouse fibroblast lineage cell at the highest concentrations tested when in acute exposure, generating reduced cell viability, oxidative stress, and cell death by apoptosis. After acute exposure and withdrawal of the stimulus (NP), the fibroblasts indicate a possible recovery for the concentration of 150 µg/mL, which is not observed for the highest concentration (250 µg/mL) since a significant decrease was observed in the ability to form colonies and cell proliferation. Such a fact may be related to the antioxidant mechanism present in the cell and triggered in the first hours of TiO₂ NP exposure, serving as protection with weak pro-apoptotic signal, and DNA repair thus reversing the apoptosis pathway in lower concentrations [20, 87].

Due to the specific amount of TiO₂ NP provided for the studies, there were limitations on the methodologies to be performed as well as the number of concentrations and exposure times tested. Therefore, future studies are needed to further investigate the effects of prolonged exposure to this TiO₂ NP in the LA-9 lineage to clarify whether this initial cytotoxicity endures resulting in damage as reported for the highest concentration (250 µg/mL) and by works using other TiO₂ NPs in different cell lines in a dose and time-dependent mechanism, or whether such effects are reversed by existing protective mechanisms in the cellular machinery [24, 43, 57].

It should also be noted that the characteristics of TiO₂ NP used in this study should be taken into account when evaluating its biological effects because although it is a small particle size (around 3.5 nm) which makes it a reactive NP, it presents functionalization with sodium carboxylate, which may contribute to its better solubility in water reducing its toxicity. The findings of this work contribute to the understanding of the acute effects of this TiO₂ NP, however, studies investigating its effects in prolonged exposures are still needed to define which cellular mechanisms are effectively involved in this possible recovery from the damage involved. In addition, we emphasize the need for standardization in future studies that facilitate the analysis and comparison of results and thus help define the degree of toxicity or not of the material under study.

Conclusion

Through the results of this work, it is possible to conclude that this TiO₂ NP, functionalized with sodium carboxylate (-COO-Na⁺), promoted cytotoxicity in LA-9 mouse fibroblasts after acute exposure, at the highest concentrations tested, 150 and 250 µg/mL. This cytotoxicity occurred through reduced viability and consequent cell death by apoptosis, probably due to oxidative stress generated by NP. It is notable that at the highest concentration (250 µg/mL) the cellular damage was not reversed, showing less clonogenic capacity even after removal of the NP. This fact emphasizes the importance of studies with different concentrations of NP since cytotoxicity is dose and time-dependent. We highlight the need for studies of prolonged exposure that help in better understanding the interaction of NP with the biological system to delineate the safety, both for health and the environment, in its use in various consumer products and the industrial sector.

Acknowledgements

We acknowledge all the people that contributed to the development of this work, the research group of Prof. Dr. Koiti Araki (University of São Paulo - USP) for his collaboration

in the synthesis of the tested nanoparticles, collaborators from the Federal University of São Carlos (UFSCar), Doctor Márcia Regina Cominetti (Department of Gerontology) for the cytometer available for our analysis and Doctor Iran Malavazi (Department of Genetics and Evolution) for all his help in obtaining the images by SEM. We also thank Doctor Eduardo Henrique Martins Nunes and M.Sc. Himad Ahmed Alcamand from the Department of Metallurgical and Materials Engineering, Federal University of Minas Gerais (UFMG) for the help in our ATR-FTIR analysis. And all the members of the Nano-PETROBRAS project team who indirectly assisted in this work.

Author Contributions

AF, PB, KF, MP, RC, YA, JR, GL and JC participated in the performance of assays and data analysis. VZ, CS, KR and FA were responsible for materials acquisition and interpretation of data. FA participated in the production of the manuscript, acquisition of funding, and coordination of the project. All authors contributed to writing or critical review of the work for intellectual content and approved the final version.

Funding Sources

This work was supported by Leopoldo Américo Miguez de Mello Research Center (CENPES-PETROBRAS). Project: Proc. No 2017/00010-7.

Disclosure Statement

The authors report no conflicts of interest in this work.

References

- 1 Auffan M, Rose J, Bottero JY, Lowry G V., Jolivet JP, Wiesner MR. Towards a definition of inorganic nanoparticles from an environmental, health and safety perspective. *Nat Nanotechnol Nature Publishing Group*; 2009;4:634–641.
- 2 Bayda S, Adeel M, Tuccinardi T, Cordani M, Rizzolio F. The history of nanoscience and nanotechnology: From chemical-physical applications to nanomedicine. *Molecules* 2020;25:1–15.
- 3 Shi H, Magaye R, Castranova V, Zhao J. Titanium dioxide nanoparticles: A review of current toxicological data. *Part Fibre Toxicol* 2013;10.
- 4 Hulla JE, Sahu SC, Hayes AW. Nanotechnology: History and future. *Hum Exp Toxicol* 2015;34:1318–1321.
- 5 Khalil M, Jan BM, Tong CW BM. Advanced nanomaterials in oil and gas industry: design, application and challenges. *Appl Energy* 2017;191:287–310.
- 6 Daniyal M, Azam A, Akhtar S. Application of Nanomaterials in Civil Engineering. *Nanomater Their Appl* 2018;169–89.
- 7 Chen X, Mao SS. Titanium dioxide nanomaterials: Synthesis, properties, modifications and applications. *Chem Rev* 2007;107:2891–2959.
- 8 Luttrell T, Halpegamage S, Tao J, Kramer A, Sutter E, Batzill M. Why is anatase a better photocatalyst than rutile? - Model studies on epitaxial TiO₂ films. *Sci Rep* 2015;4:4043
- 9 Zhang X, Li W, Yang Z. Toxicology of nanosized titanium dioxide: an update. *Arch Toxicol Springer Berlin Heidelberg*; 2015;89:2207–2217.
- 10 Johnson HA, Williamson RS, Marquart M, Bumgardner JD, Janorkar A V., Roach MD. Photocatalytic activity and antibacterial efficacy of UVA-treated titanium oxides. *J Biomater Appl* 2020;35:500–14.
- 11 Bernier M-C, El Kirat K, Besse M, Morandat S, Vayssade M. Preosteoblasts and fibroblasts respond differently to anatase titanium dioxide nanoparticles: A cytotoxicity and inflammation study. *Colloids Surfaces B Biointerfaces Elsevier B.V.*; 2012;90:68–74.

- 12 Negi GS, Anirbid S, Sivakumar P. Applications of silica and titanium dioxide nanoparticles in enhanced oil recovery: Promises and challenges. *Pet Res Elsevier Ltd*; 2021;6:224–246.
- 13 Panahpoori D, Rezvani H, Parsaei R, Riazi M. A pore-scale study on improving CTAB foam stability in heavy crude oil–water system using TiO₂ nanoparticles. *J Pet Sci Eng Elsevier B.V.*; 2019;183:106411.
- 14 Nowrouzi I, Khaksar Manshad A, Mohammadi AH. Effects of MgO, γ -Al₂O₃, and TiO₂ Nanoparticles at Low Concentrations on Interfacial Tension (IFT), Rock Wettability, and Oil Recovery by Spontaneous Imbibition in the Process of Smart Nanofluid Injection into Carbonate Reservoirs. *ACS Omega* 2022;7:22161–2272.
- 15 Topare NS, Joy M, Joshi RR, Jadhav PB, Kshirsagar LK. Treatment of petroleum industry wastewater using TiO₂/UV photocatalytic process. *J Indian Chem Soc* 2015;92:219–222.
- 16 Ani IJ, Akpan UG, Olutoye MA, Hameed BH. Photocatalytic degradation of pollutants in petroleum refinery wastewater by TiO₂- and ZnO-based photocatalysts: Recent development. *J Clean Prod Elsevier Ltd*; 2018;205:930–954.
- 17 Dhawale DS, Gujar TP, Lokhande CD. TiO₂ Nanorods Decorated with Pd Nanoparticles for Enhanced Liquefied Petroleum Gas Sensing Performance. *Anal Chem* 2017;89:8531–8537.
- 18 Rosestolato JCS, Pérez-Gramatges A, Lachter ER, Nascimento RSV. Lipid nanostructures as surfactant carriers for enhanced oil recovery. *Fuel Elsevier*; 2019;239:403–412.
- 19 Ibrahim M, Schoelermann J, Mustafa K, Cimpan MR. TiO₂ nanoparticles disrupt cell adhesion and the architecture of cytoskeletal networks of human osteoblast-like cells in a size dependent manner. *J Biomed Mater Res Part A* 2018;106:2582–2593.
- 20 Gholinejad Z, Khadem Ansari MH, Rasmi Y. Titanium dioxide nanoparticles induce endothelial cell apoptosis via cell membrane oxidative damage and p38, PI3K/Akt, NF- κ B signaling pathways modulation. *J Trace Elem Med Biol Elsevier*; 2019;54:27–35.
- 21 Wang Y, Yao C, Li C, Ding L, Liu J, Dong P, Fang H, Lei Z, Shi G, Wu M. Excess titanium dioxide nanoparticles on the cell surface induce cytotoxicity by hindering ion exchange and disrupting exocytosis processes. *Nanoscale* 2015;7:13105–15.
- 22 Soto Veliz D, Luoto JC, Pulli I, Toivakka M. The influence of mineral particles on fibroblast behaviour: A comparative study. *Colloids Surfaces B Biointerfaces Elsevier B.V.*; 2018;167:239–51
- 23 Pedrino M, Brassolatti P, Maragno Fattori AC, Bianchi J, de Almeida Rodolpho JM, de Godoy KF, Assis M, Longo E, Nogueira Zambone Pinto Rossi K, Speglich C, de Freitas Anibal F. Analysis of cytotoxicity and genotoxicity in a short-term dependent manner induced by a new titanium dioxide nanoparticle in murine fibroblast cells. *Toxicol Mech Methods Taylor & Francis*; 2022;32:213–23.
- 24 Brassolatti P, de Almeida Rodolpho JM, Franco de Godoy K, de Castro CA, Flores Luna GL, Dias de Lima Fragelli B, Pedrino M, Assis M, Nani Leite M, Cancino-bernardi J, Speglich C, Frade MA, Anibal FDF. Functionalized Titanium Nanoparticles Induce Oxidative Stress and Cell Death in Human Skin Cells. *Int J Nanomedicine* 2022;Volume 17:1495–509.
- 25 Ghosh M, Chakraborty A, Mukherjee A. Cytotoxic, genotoxic and the hemolytic effect of titanium dioxide (TiO₂) nanoparticles on human erythrocyte and lymphocyte cells in vitro. *J Appl Toxicol* 2013;33:1097–110.
- 26 Liu N, Tang M. Toxic effects and involved molecular pathways of nanoparticles on cells and subcellular organelles. *J Appl Toxicol* 2020;40:16–36.
- 27 Mohammadinejad R, Moosavi MA, Tavakol S, Vardar DÖ, Hosseini A, Rahmati M, Dini L, Hussain S. Mandegary A, Klionsky D. Necrotic, apoptotic and autophagic cell fates triggered by nanoparticles. *Autophagy Taylor & Francis*; 2019;15:4–33.
- 28 Dai X, Liu R, Li N, Yi J. Titanium dioxide nanoparticles induce in vitro autophagy. *Hum Exp Toxicol* 2019;38:56–64.

- 29 Prokopiuk V, Yefimova S, Onishchenko A, Kapustnik V, Myasoedov V, Maksimchuk P, Butov D, Bepalova I, Tkachenko A. Assessing the Cytotoxicity of TiO₂-x Nanoparticles with a Different Ti³⁺/(Ti²⁺)/Ti⁴⁺ Ratio. *Biol Trace Elem Res* 2022.
- 30 Shukla RK, Kumar A, Gurbani D, Pandey AK, Singh S, Dhawan A. TiO₂ nanoparticles induce oxidative DNA damage and apoptosis in human liver cells. *Nanotoxicology* 2013;7:48–60.
- 31 Tomankova K, Horakova J, Harvanova M, Malina L, Soukupova J, Hradilova S, Kejlova K, Malohlava J, Licman L, Dvorakova M, Jirova D, Kolarova H. Cytotoxicity, cell uptake and microscopic analysis of titanium dioxide and silver nanoparticles in vitro. *Food Chem Toxicol Elsevier Ltd*; 2015;82:106–15.
- 32 Kim KT, Klaine SJ, Cho J, Kim S-H, Kim SD. Oxidative stress responses of *Daphnia magna* exposed to TiO₂ nanoparticles according to size fraction. *Sci Total Environ* 2010;408:2268–72.
- 33 Gholinejad Z, Khadem Ansari MH, Rasmi Y. Titanium dioxide nanoparticles induce endothelial cell apoptosis via cell membrane oxidative damage and p38, PI3K/Akt, NF-κB signaling pathways modulation. *J Trace Elem Med Biol Elsevier*; 2019;54:27–35.
- 34 Li Z, He J, Li B, Zhang J, He K, Duan X, Huang R, Wu Z, Xiang G. Titanium dioxide nanoparticles induce endoplasmic reticulum stress-mediated apoptotic cell death in liver cancer cells. *J Int Med Res* 2020;48:030006052090365.
- 35 Murugadoss S, Brassinne F, Sebaihi N, Petry J, Cokic SM, Van Landuyt KL, Godderis L, Mast J, Lison D, Hoet P, Van den Brule S. Agglomeration of titanium dioxide nanoparticles increases toxicological responses in vitro and in vivo. *Part Fibre Toxicol Particle and Fibre Toxicology*; 2020;17:10.
- 36 Hamed MT, Bakr BA, Shahin YH, Elwakil BH, Abu-Serie MM, Aljohani FS, Bekhit AA. Novel Synthesis of Titanium Oxide Nanoparticles: Biological Activity and Acute Toxicity Study. *Keramidas A, editor. Bioinorg Chem Appl* 2021;2021:1–14.
- 37 Wall J, Seleci DA, Schworm F, Neuberger R, Link M, Hufnagel M, Schumacher P, Schulz F, Heinrich U, Wohlleben W, Hartwig A. Comparison of Metal-Based Nanoparticles and Nanowires: Solubility, Reactivity, Bioavailability and Cellular Toxicity. *Nanomaterials* 2021;12:147.
- 38 Lee SH, Won H, Kim S-H, Jeon S, Jeong J, Lee D-K, Yang J-Y, Seok J-H, Jung K, Oh JH, Lee JH, Cho W-S. Six-well plate-based colony-forming efficacy assay and Co-Culture application to assess toxicity of metal oxide nanoparticles. *Regul Toxicol Pharmacol* 2022;128:105085.
- 39 Mosmann T. Rapid colorimetric assay for cellular growth and survival: application to proliferation and cytotoxicity assays. *J Immunol Methods* 1983;65:55–63.
- 40 Jin C-Y, Zhu B-S, Wang X-F, Lu Q-H. Cytotoxicity of Titanium Dioxide Nanoparticles in Mouse Fibroblast Cells. *Chem Res Toxicol* 2008;21:1871–7.
- 41 Zhang J, Song W, Guo J, Zhang J, Sun Z, Li L, Ding F, Gao M. Cytotoxicity of different sized TiO₂nanoparticles in mouse macrophages. *Toxicol Ind Health* 2013;29:523–33.
- 42 Hamzeh M, Sunahara GI. In vitro cytotoxicity and genotoxicity studies of titanium dioxide (TiO₂) nanoparticles in Chinese hamster lung fibroblast cells. *Toxicol Vitro* 2013;27:864–73.
- 43 Coccini T, Grandi S, Lonati D, Locatelli C, De Simone U. Comparative cellular toxicity of titanium dioxide nanoparticles on human astrocyte and neuronal cells after acute and prolonged exposure. *Neurotoxicology Elsevier B.V.*; 2015;48:77–89.
- 44 Tripathi VK, Sivakumar AS, Dhasmana A, Hwang I. Crosstalk Between Co-Cultured 3T3-L1 and C2C12 Cells After the Exposure of Nano-Titanium Dioxide. *J Nanosci Nanotechnol* 2018;18:3870–9.
- 45 Franken NAP, Rodermond HM, Stap J, Haveman J, van Bree C. Clonogenic assay of cells in vitro. *Nat Protoc* 2006;1:2315–9.
- 46 Wan CP, Myung E, Lau BHS. An automated micro-fluorometric assay for monitoring oxidative burst activity of phagocytes. *J Immunol Methods* 1993;159:131–8.

- 47 Wang H, Joseph JA. Quantifying cellular oxidative stress by dichlorofluorescein assay using microplate reader. *Mention of a trade name, proprietary product, or specific equipment does not constitute a guarantee by the United States Department of Agriculture and does not imp.* *Free Radic Biol Med* 1999;27:612–6.
- 48 Nel AE, Mädler L, Velegol D, Xia T, Hoek EMV, Somasundaran P, Klaessig F, Castranova V, Thompson M. Understanding biophysicochemical interactions at the nano-bio interface. *Nat Mater Nature Publishing Group*; 2009;8:543–57.
- 49 Nguyen VH, Lee BJ. Protein corona: A new approach for nanomedicine design. *Int J Nanomedicine* 2017;12:3137–51.
- 50 Maiorano G, Sabella S, Sorce B, Brunetti V, Malvindi MA, Cingolani R, Pompa PP. Effects of cell culture media on the dynamic formation of protein-nanoparticle complexes and influence on the cellular response. *ACS Nano* 2010;4:7481–91.
- 51 Shukla RK, Sharma V, Pandey AK, Singh S, Sultana S, Dhawan A. ROS-mediated genotoxicity induced by titanium dioxide nanoparticles in human epidermal cells. *Toxicol Vitr Elsevier Ltd*; 2011;25:231–41.
- 52 Arvizo RR, Miranda OR, Thompson MA, Pabelick CM, Bhattacharya R, David Robertson J, Rotello VM, Prakash YS, Mukherjee P. Effect of nanoparticle surface charge at the plasma membrane and beyond. *Nano Lett* 2010;10:2543–8.
- 53 Singh BP, Menchavez R, Takai C, Fuji M, Takahashi M. Stability of dispersions of colloidal alumina particles in aqueous suspensions. *J Colloid Interface Sci* 2005;291:181–6.
- 54 Nurdin I, Johan MR, Yaacob II, Ang BC. Effect of nitric acid concentrations on synthesis and stability of maghemite nanoparticles suspension. *Sci World J* 2014;2014.
- 55 Hamilton RF, Wu N, Xiang C, Li M, Yang F, Wolfarth M, Porter DW, Holian A. Synthesis, characterization, and bioactivity of carboxylic acid-functionalized titanium dioxide nanobelts. *Part Fibre Toxicol* 2014;11:1–15.
- 56 Hou Y, Lai M, Chen X, Li J, Hu Y, Luo Z, Ding X, Cai K. Effects of mesoporous SiO₂, Fe₃O₄, and TiO₂ nanoparticles on the biological functions of endothelial cells in vitro. *J Biomed Mater Res Part A* 2014;102:1726–36.
- 57 Uboldi C, Urbán P, Gilliland D, Bajak E, Valsami-Jones E, Ponti J, Rossi F. Role of the crystalline form of titanium dioxide nanoparticles: Rutile, and not anatase, induces toxic effects in Balb/3T3 mouse fibroblasts. *Toxicol Vitr The Authors*; 2016;31:137–45.
- 58 Mudunkotuwa IA, Minshid A Al, Grassian VH. ATR-FTIR spectroscopy as a tool to probe surface adsorption on nanoparticles at the liquid–solid interface in environmentally and biologically relevant media. *Analyst* 2014;139:870–81.
- 59 Almeida NA, Martins PM, Teixeira S, Lopes da Silva JA, Sencadas V, Kühn K, Cuniberti G, Lanceros-Mendez S, Marques PAAP. TiO₂/graphene oxide immobilized in P(VDF-TrFE) electrospun membranes with enhanced visible-light-induced photocatalytic performance. *J Mater Sci* 2016;51:6974–86.
- 60 Praveen P, Viruthagiri G, Mugundan S, Shanmugam N. Structural, optical and morphological analyses of pristine titanium di-oxide nanoparticles – Synthesized via sol–gel route. *Spectrochim Acta Part A Mol Biomol Spectrosc Elsevier B.V.*; 2014;117:622–9.
- 61 Nadimi M, Ziarati Saravani A, Aroon MA, Ebrahimian Pirbazari A. Photodegradation of methylene blue by a ternary magnetic TiO₂/Fe₃O₄/graphene oxide nanocomposite under visible light. *Mater Chem Phys Elsevier*; 2019;225:464–74.
- 62 Zhang H-X, He X-D, He F. Microstructural characterization and properties of ambient-dried SiO₂ matrix aerogel doped with opacified TiO₂ powder. *J Alloys Compd* 2009;469:366–9.
- 63 Rajakumar G, Rahuman AA, Roopan SM, Khanna VG, Elango G, Kamaraj C, Zahir AA, Velayutham K. Fungus-mediated biosynthesis and characterization of TiO₂ nanoparticles and their activity against pathogenic bacteria. *Spectrochim Acta Part A Mol Biomol Spectrosc Elsevier B.V.*; 2012;91:23–9.

- 64 Sun D, Yang J, Wang X. Bacterial cellulose/TiO₂ hybrid nanofibers prepared by the surface hydrolysis method with molecular precision. *Nanoscale* 2010;2:287–92.
- 65 Maurya IC, Neetu, Gupta AK, Srivastava P, Bahadur L. Callindra haematocephata and Peltophorum pterocarpum flowers as natural sensitizers for TiO₂ thin film based dye-sensitized solar cells. *Opt Mater (Amst)* 2016;60:270–6.
- 66 Singh LK, Koiry BP. Natural Dyes and their Effect on Efficiency of TiO₂ based DSSCs: a Comparative Study. *Mater Today Proc Elsevier Ltd*; 2018;5:2112–22.
- 67 Guo X, Li X, Qin L, Kang S-Z, Li G. A highly active nano-micro hybrid derived from Cu-bridged TiO₂/porphyrin for enhanced photocatalytic hydrogen production. *Appl Catal B Environ Elsevier*; 2019;243:1–9.
- 68 Zhuang B, Xiangqing L, Ge R, Kang S, Qin L, Li G. Assembly and electron transfer mechanisms on visible light responsive 5, 10, 15, 20-meso-tetra(4-carboxyphenyl) porphyrin/cuprous oxide composite for photocatalytic hydrogen production. *Appl Catal A Gen Elsevier B.V.*; 2017;533:81–9.
- 69 Dao TH, Tran TT, Nguyen VR, Pham TNM, Vu CM, Pham TD. Removal of antibiotic from aqueous solution using synthesized TiO₂ nanoparticles: characteristics and mechanisms. *Environ Earth Sci Springer Berlin Heidelberg*; 2018;77:359.
- 70 Mirghani MES, Che Man YB, Jinap S, Baharin BS, Bakar J. FTIR spectroscopic determination of soap in refined vegetable oils. *J Am Oil Chem Soc* 2002;79:111–6.
- 71 Mei BC, Susumu K, Medintz IL, Mattoussi H. Polyethylene glycol-based bidentate ligands to enhance quantum dot and gold nanoparticle stability in biological media. *Nat Protoc* 2009;4:412–23.
- 72 Arami H, Khandhar A, Liggitt D, Krishnan KM. In vivo delivery, pharmacokinetics, biodistribution and toxicity of iron oxide nanoparticles. *Chem Soc Rev* 2015;44:8576–607.
- 73 Varanda LC, De Souza CGS, Perecin CJ, De Moraes DA, De Queiróz DF, Neves HR, Junior JBS, Da Silva MF, Albers RF, Da Silva TL. Inorganic and organic-inorganic composite nanoparticles with potential biomedical applications: Synthesis challenges for enhanced performance. *Mater. Biomed. Eng. Bioact. Mater. Prop. Appl* 2019.
- 74 Kalluri R, Zeisberg M. Fibroblasts in cancer. *Nat Rev Cancer* 2006;6:392–401.
- 75 Zhang XQ, Yin LH, Tang M, Pu YP. ZnO, TiO₂, SiO₂, and Al₂O₃ nanoparticles-induced toxic effects on human fetal lung fibroblasts. *Biomed Environ Sci* 2011;24:661–9.
- 76 Allouni ZE, Høl PJ, Cauqui MA, Gjerdet NR, Cimpan MR. Role of physicochemical characteristics in the uptake of TiO₂ nanoparticles by fibroblasts. *Toxicol Vitro Elsevier Ltd*; 2012;26:469–79.
- 77 Lee S-U, Lee J-E, Kim S-J, Lee J-S. Effects of titanium dioxide nanoparticles on the inhibition of cellular activity in human Tenon's fibroblasts under UVA exposure. *Graefe's Arch Clin Exp Ophthalmol Graefe's Archive for Clinical and Experimental Ophthalmology*; 2018;256:1895–903.
- 78 Setyawati MI, Sevensan C, Bay BH, Xie J, Zhang Y, Demokritou P, Leong DT. Nano-TiO₂ Drives Epithelial-Mesenchymal Transition in Intestinal Epithelial Cancer Cells. *Small* 2018;14:1800922.
- 79 Elango J, Selvaganapathy PR, Lazzari G, Bao B, Wenhui W. Biomimetic collagen-sodium alginate-titanium oxide (TiO₂) 3D matrix supports differentiated periodontal ligament fibroblasts growth for periodontal tissue regeneration. *Int J Biol Macromol Elsevier B.V.*; 2020;163:9–18.
- 80 Song B, Zhang Y, Liu J, Feng X, Zhou T, Shao L. Unraveling the neurotoxicity of titanium dioxide nanoparticles: focusing on molecular mechanisms. *Beilstein J Nanotechnol* 2016;7:645–54.
- 81 Hirakawa K, Mori M, Yoshida M, Oikawa S, Kawanishi S. Photo-irradiated Titanium Dioxide Catalyzes Site Specific DNA Damage via Generation of Hydrogen Peroxide. *Free Radic Res* 2004;38:439–47.
- 82 Chen T, Yan J, Li Y. Genotoxicity of titanium dioxide nanoparticles. *J Food Drug Anal Elsevier Masson SAS*; 2014;22:95–104.

- 83 Han SG, Newsome B, Hennig B. Titanium dioxide nanoparticles increase inflammatory responses in vascular endothelial cells. *Toxicology* Elsevier Ireland Ltd; 2013;306:1–8.
- 84 Buechler MB, Turley SJ. A short field guide to fibroblast function in immunity. *Semin Immunol* Elsevier; 2018;35:48–58.
- 85 Vandebriel RJ, Vermeulen JP, van Engelen LB, de Jong B, Verhagen LM, de la Fonteyne-Blankestijn LJ, Hoonakker ME, de Jong WH. The crystal structure of titanium dioxide nanoparticles influences immune activity in vitro and in vivo. *Part Fibre Toxicol Particle and Fibre Toxicology*; 2018;15:9.
- 86 Wang J. DNA damage and apoptosis. *Cell Death Differ* 2001;8:1047–8.
- 87 Elmore S. Apoptosis: A Review of Programmed Cell Death. *Toxicol Pathol* 2007;35:495–516.
- 88 L Browning C. Titanium Dioxide Nanoparticles are not Cytotoxic or Clastogenic in Human Skin Cells. *J Environ Anal Toxicol* 2014;04.
- 89 OECD. Evaluation of in vitro methods for human hazard assessment applied in the OECD Testing Programme for the Safety of Manufactured Nanomaterials - Series on the Safety of Manufactured Nanomaterials, No. 85 . 2018.